Anomalous influence of high-frequency ultrasound on radiation diffraction in deformed single crystals

E. M. Iolin, E. A. Raĭtman, B. V. Kuvaldin, and É. V. Zolotoyabko

Physics Institute, Latvian Academy of Sciences

Results are reported of the study of neutron and x-ray diffraction in deformed single crystals excited by high-frequency ultrasound. It is shown theoretically that ultrasound of frequency above a certain threshold violates the adiabaticity condition for the motion of the representative points over the sheets of the dispersion surface. This results in an anomalous (compared with diffraction by an ideal crystal) dependence of the scattering intensity on the ultrasound-wave amplitude. The experimental data obtained for silicon crystals agree well with the theoretical predictions.

1. INTRODUCTION

The effect of ultrasound (US) on neutron and x-ray scattering in perfect crystals has been the subject of many investigations. Their result reduce mainly to the following: In the long-wave limit ($\lambda_s \ll \tau$, where λ_s is the US wavelength, $\tau = 2\pi/\Delta k_0$ the extinction length, and Δk_0 the gap between the sheets of the dispersion surface (DS) for the Bloch states of a radiation quantum in the crystal), the spatial periodicity of the displacement wave is hardly manifested in the scattering, and US leads to an increase of the diffraction intensity I all the way to the kinematic limit, on account of the spreading of the angle interval and of the interval of the wavelengths λ for Bragg reflection (see, e.g., Refs. 1 and 2). The US is equivalent in this case to a smooth but time-dependent lattice deformation. If $\lambda_s < \tau$, the US mixes the states corresponding to different sheets of the DS, producing on the latter self-intersection points at which new gaps Δk_s appear and take, for symmetric reflection, the form

$$\Delta k_s = \Delta k_0 |\mathbf{Hw}|, \qquad (1)$$

where **H** is the reciprocal-lattice vector, **w** the US amplitude, and $\Delta k_s \ll \Delta k_0$ for $|\mathbf{H \cdot w}| \ll 1$ (Ref. 3). The presence of the additional gaps Δk_s leads to a number of effects, particularly to Pendellösung beats of the diffraction intensity I as a function of w. These beats were predicted theoretically in Ref. 4 and were observed experimentally in diffraction of neutrons[5,6] and of x rays.[7]

In a perfect crystal, neglecting the I(w) oscillations, high-frequency US also increases the scattering intensity, albeit in accordance with a somewhat different law than for the case $\lambda_s \gg \tau$ (Refs. 4 and 8). We call this behavior normal, since it is typical of most situations. An exception is the observed decrease of the intensity I(w) in thick crystals ($\mu T \gg 1$, where μ is the absorption coefficient and T the sample thickness), due to US "disruption" of Borrmann origin, which is particularly effective under conditions of neutron-acoustic[9] and x-ray-acoustic[10] resonance ($\lambda_s \approx \tau$). Since in our experiments $\mu T \ll 1$ for neutrons and $\mu T \lesssim 1$ for x rays, the role of the Borrmann effect is insignificant.

In deformed crystals, which are of great practical interest, the effect of US on diffraction has been much less investigated. By way of example of the few studies we point to an investigation[11] carried out under conditions of low-frequency ($\nu_s \sim 1$ kHz) US excitation. The diffraction can be described in this case by quasi-classical theories (Refs. 13–14), but with account taken of the time dependence of the US diplacements. The effects observed are small, since US with $\lambda_s \gg \tau$ exerts in a deformed crystal a weak influence on the Bragg-reflection conditions.

We report here the results of theoretical and experimental investigations of neutron and x-ray diffraction in deformed crystals under hf ($\lambda_s < \tau$) US excitation. We show for the first time ever that high-frequency US leads to violation of the adiabaticity conditions for the motion of the representative sheets of the DS in smoothly deformed crystals. The result is an anomalous dependence of the diffraction intensity I on the US amplitude w, a dependence characterized by a substantial (up to 50%) decrease of I(w) for small w. Next, with increase of w, the intensity I(w) increases linearly and reaches in final analysis the kinematic limit. A notrivial fact is that in absolute numbers the influence of the US is much more strongly manifested in diffraction in a strained crystal than for an ideal lattice. Owing to the static strain, a substantial role is played by multiphoton processes even at small w.

Anomalous I(w) dependences were observed by us in experiments on neutron and x-ray scattering. The experimental data agree well with the theoretical predictions.

The presence of a static strain leads also to appearance of a new type of Pendellösung beats in hf US excitation, and furthermore under conditions when ordinary extinction beats (including those connected with the gaps Δk_s) are already suppressed.

2. THEORY

2.1. General formulation. Single-photon transitions

At US frequencies ν_s exceeding the threshold[1)] ν_{th}, when the DS sheets intersect and new gaps Δk_s (1) appear, the scattering process is determined in many respects by the relation between the usual extinction length and the "sonic" one $\tau_s = \tau/|\mathbf{H \cdot w}|$. It is important that at small $|\mathbf{H \cdot w}| \ll 1$ the length τ_s can become much larger than τ (τ_s is actually limited by the crystal thickness T). For example, $\tau_s/\tau \approx 10$ in the experiments of Refs. 6 and 7 and $\tau_s/\tau \approx 60$ in Ref. 5. By virtue of this circumstance, the diffraction in the presence of US is more sensitive to lattice strain compared with ordinary Bragg scattering.

We introduce the characteristic length λ_d over which

the strain δ changes noticeably (λ_{ij} grad $\delta \sim \delta$). At $\lambda_d \ll \tau_s$ the role of the static distortions reduces to renormalization (to an increase of τ_s) and the influence of the US on the diffraction is, generally speaking, decreased. The strongest action of structure distortions on US diffraction effects should be observed at $\lambda_d \approx \tau_s$. Deferring this "threshold" situation to a separate consideration, we analyze in greater detail the case of smooth deformations ($\lambda_d > T$). To be definite, we consider symmetric Laue reflection in a thick single-crystal plate ($T \gg \tau$), which accords with our experimental conditions. The calculations were carried out for neutron diffraction, but with an obvious change of notation the equations are valid also for x-ray scattering, at any rate for weak absorption ($\mu T \lesssim 1$).

In the two-way approximation, the propagation of a neutron wave in a deformed crystal is described by an equation of the Takagi type[15]:

$$\frac{i}{v_n}\frac{\partial \psi_0}{\partial t} = -i\frac{\partial \psi_0}{\partial s_0} + \frac{\Delta k_0}{2}\cos\theta_B \exp(iH\mathbf{u}_s)\psi_h,$$
(2)

$$\frac{i}{v_n}\frac{\partial \psi_h}{\partial t} = -i\frac{\partial \psi_h}{\partial s_h} - \frac{\partial(H\mathbf{u}_d)\psi_h}{\partial s_h} + \frac{\Delta k_0}{2}\cos\theta_B \exp(-iH\mathbf{u}_s)\psi_0,$$

$$\mathbf{k}_h = \mathbf{k}_0 + \mathbf{H}, \qquad k_h{}^2 = k_0{}^2,$$

where ψ_0, $\psi_h \exp(-iH\mathbf{u}_d)$, $\mathbf{k}_0$ and $\mathbf{k}_h$ are the amplitudes and wave vectors of the incident and diffracted waves; s_0 and s_h are the coordinates along $\mathbf{k}_0$ and $\mathbf{k}_h$; m and v_n are the neutron mass and velocity; θ_B is the Bragg angle; $\mathbf{u}_d$ and $\mathbf{u}_s$ are the static and US displacements of the nucleus. In the general case of smooth deformations in the scattering plane, the integral intensities can be calculated by assuming[14]

$$H\mathbf{u}_d = 4bs_0 s_h,$$
(3)

where b is a constant. We confine ourselves to the case $|b| \ll \Delta k_0{}^2$, when the scattering intensity is much lower than the kinematic limit. Each point of the crystal has then its own two-sheet DS, and the neutron moves adiabatically inside the crystal and adjusts itself to the DS without transitions between the sheets. As shown in Ref. 12, the diffraction process can be described within the framework of a single DS, but as the neutron penetrates into the sample the representative points of the excitations move over the DS sheets in the directions shown by the arrows (for $b > 0$) in Fig. 1. We emphasize that the component of the point velocity along the x axis are equal in magnitude and sign for both DS sheets. The role of US in such a scheme, as shown below, is mainly to stimulate transitions between the DS sheets. (A more detailed further theoretical analysis is contained in Ref. 16.)

Let a transverse US wave propagate along the z axis perpendicular to the crystal surface, with a displacement $\mathbf{w} \| \mathbf{x}$:

$$\mathbf{u}_s = \mathbf{w}\exp[i(k_s z - \omega_s t)] + \text{c.c.}, \quad k_s = 2\pi/\lambda_s, \quad \omega_s = 2\pi\nu_s. \quad (4)$$

Starting with the system (2), we obtain in the one-phonon approximation for the wave-function components $\psi_{0,h}(\alpha)$ (corresponding to the absorption of $\alpha = 0$ and ± 1 US phonons)

$$\begin{pmatrix} \alpha\Omega + i\dfrac{\partial}{\partial S_0} & -1 \\ -1 & \alpha\Omega + i\dfrac{\partial}{\partial S_h} + 4BS_0 \end{pmatrix}|\psi(\alpha)\rangle$$
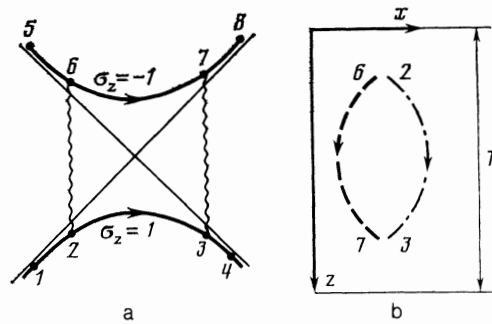
FIG. 1. Dynamics of motion of the excitation points in a deformed crystal: a—in momentum space; b—in coordinate space

$$= |Hw| \begin{pmatrix} 0 & -i \\ i & 0 \end{pmatrix} \sum_{\beta = \pm 1} |\psi(\alpha - \beta)\rangle,$$
(5)

$$|\psi(\alpha)\rangle \equiv \begin{vmatrix} \psi_0(\alpha) \\ \psi_h(\alpha) \end{vmatrix},$$

where we have introduced the dimensionless quantities

$$\Omega = \left(\frac{\omega_s}{v_n} + k_s\cos\theta_B\right)\left(\frac{\Delta k_0}{2}\cos\theta_B\right)^{-1}, \quad S_{0,h} = s_{0,h}\frac{\Delta k_0}{2}\cos\theta_B,$$

$$|B| = |b|\left(\frac{\Delta k_0}{2}\cos\theta_B\right)^{-2} \ll 1, \quad T' = T\frac{\Delta k_0}{2}\cos\theta_B \gg 1,$$

$$P_{0,h} = p_{0,h}\left(\frac{\Delta k_0}{2}\cos\theta_B\right)^{-1},$$

$p_{0,k}$ are the wave-packet momenta conjugate to the coordinates $s_{0,h}$ (the quantity p_h is conserved). For $Hw \ll 1$ we can confine ourselves to a pair of states $|\psi(\alpha)\rangle$ and $|\psi(\alpha - \beta)\rangle$ that interact with the aid of the US perturbation. The transitions $|\psi(\alpha)\rangle \leftrightarrow |\psi(\alpha - \beta)\rangle$ between the DS sheets take place in the vicinity of the points $s_0 = s_s^*$ corresponding to the momenta $p_0 = p_0^*$:

$$P_0^* = (2\alpha - \beta)\Omega/2 - r_1[(\Omega/2)^2 - 1]^{1/2},$$
$$P_h^* - 4BS_0^* = (2\alpha - \beta)\Omega/2 + r_1[(\Omega/2)^2 - 1]^{1/2}.$$
(6)

The values $r_1 = \pm 1$ in (6) correspond to transitions at points separated in space by a distance

$$\Delta S = \frac{1}{2B}\left[\left(\frac{\Omega}{2}\right)^2 - 1\right]^{1/2}.$$
(7)

Eliminating $\psi_h(\alpha)$ and $\psi_h(\alpha - \beta)$ from (5) and expanding the coefficients in a series in $S_0 - S_0^*$ up to the first nonvanishing term, we obtain for the functions $\Phi(\alpha)$ and $\Phi_0(\alpha - \beta)$, which are proportional to $\psi_0(\alpha)$ and $\psi_0(\alpha - \beta)$, the equations

$$\left[i\frac{\partial}{\partial S_0} + 2B(Q_\alpha^{-2} + Q_{\alpha-\beta}^{-2})(S_0 - S_0^*)\right]$$

$$\Phi_0(\alpha) - i|Hw|\beta\Omega\Phi_0(\alpha - \beta) = 0,$$

$$\left[i\frac{\partial}{\partial S_0} - 2B(Q_\alpha^{-2} + Q_{\alpha-\beta}^{-2})(S_0 - S_0^*)\right]$$

$$\Phi_0(\alpha - \beta) + i|Hw|\beta\Omega\Phi_0(\alpha) = 0,$$
(8)

$$Q_\alpha = \alpha\Omega - P_h + 4BS_0^*, \quad Q_\alpha Q_{\alpha-\beta} = -1.$$

The solutions of Eq. (8) are expressed in terms of the para-

bolic-cylinder functions D_v (Ref. 17):

$$\Phi_{0r}(\alpha) = D_v [r(1+i)(S_0 - S_0^*)\xi^{-1}], \quad r = \pm 1,$$
$$\nu = -\tfrac{1}{2}[1 + \text{sgn}(r_1\beta) + i(Hw\Omega\xi)^2],$$
$$\xi^{-1} = (4B\Omega)^{1/4}[(\Omega/2)^2 - 1]^{1/4}, \tag{9}$$

$$\Phi_{0r}(\alpha - \beta) = -[r(1+i)/Hw\beta\Omega\xi]D_{\nu+1}[r(1+i)(S_0 - S_0^*)\xi^{-1}], \quad \text{sgn}(r_1\beta) > 0,$$
$$\Phi_{0r}(\alpha - \beta) = [r(1+i)/Hw\beta\Omega\xi]D_{\nu-1}[r(1-i)(S_0 - S_0^*)\xi^{-1}], \quad \text{sgn}(r_1\beta) < 0.$$

The most lucid answer is obtained by using asymptotes of the functions $D_p(z)$. For $|p| \to \infty$, $|z| < |p|^{1/2}$, $\arg(-p) \leqslant \pi/2$ we have

$$D_p(z) \approx 2^{-1/4} \exp\left[\tfrac{1}{4}p \ln(-p) - \tfrac{1}{2}p - z(-p)^{1/2}\right]. \tag{10}$$

For $|z| \to \infty$, $|z| \gg |p|$,

$$D_p(z) \approx z^p \exp(-z^2/4), \quad -\pi/4 < \arg z < 3\pi/4,$$

$$D_p(z) \approx z^p \exp\left(-\frac{z^2}{4}\right) - \frac{(2\pi)^{1/2}}{\Gamma(-p)}\exp(-p\pi i)z^{-p-1}\exp\left(\frac{z^2}{4}\right),$$

$$-\frac{5\pi}{4} < \arg z < -\frac{\pi}{4}. \tag{11}$$

Let us consider several limiting cases, assuming that $HwT' \gg 1$ (multiple scattering regime, $T/\tau_s \gg 1$).

1. $B^{1/2}T' \ll 1$. The orientation of the reflecting planes changes over a thickness T by an amount $\Delta\theta \sim BT' \ll Hw\Delta\theta_0$ which is the width of the one-photon satellite $\Delta\theta_0 = \Delta k_0/H$ is the angular width of the principal reflection). The US will therefore have the same influence on the scattering as in a perfect crystal.

2. $B^{1/2}T' \gg 1$ but $BT' \ll 1$. The static strain influences little the diffraction intensity I_d ($\Delta I_d = I_d - I_0 \sim \Delta\theta_0(BT')^2 \ll 1$, where I_0 in the intensity of diffraction from an ideal crystal without US. For $Hw \ll B^{3/4}(T')^{1/2}$ we find on the basis of (11) that during the time of passage of the wave $|\psi(\alpha)\rangle$ through the crystal the excitation point has probability R_1 of remaining on the same DS sheet and a probability M_1 of going over to a state $|\psi(\alpha - \beta)\rangle$ on another sheet:

$$R_1 = \exp[-\pi(Hw\Omega\xi)^2], \quad M_1 = 1 - R_1. \tag{12}$$

$M_1 \approx 0$ if $H(w)^2 \ll B$ and $M_1 \approx 1$ if $(Hw)^2 \gg B$. These results can be illustrated qualitatively as follows. The position of the phonon satellites shifts in a deformed crystal by an amount $\Delta\theta \approx \Delta\theta_0 \cdot 2\pi B/Hw$ (over a length τ_s). If $\Delta\theta$ is less than the angular width $\Delta\theta_0 Hw$ of the satellite, the DS modified by the US are the same for an ideal and a distorted crystal (in the vicinity of S_0^*). The excitation point moves adiabatically over the DS and goes over into a state $|\psi(\alpha - \beta)\rangle$ with probability $M_1 \approx 1$.

As the neutron passes through the crystal, the change of the quasimomentum component along the x axis is of the order of $BT'\Delta k_0 \ll \Delta k_0$. The US therefore influences the dynamics of only those states that are excited near the points 2, 6, 3, and 7 (Fig. 1a). By simple calculations we find the intensity change ΔI_s due to the US, compared with the intensity $I_0 = \tfrac{1}{2}\pi\Delta\theta_0$ if the diffraction from an ideal crystal:

$$\frac{\Delta I_s}{I_0} = \frac{8BT'}{\pi\cos\theta_B}(1 - R_1)\left[1 - \left(\frac{2}{\Omega}\right)^2\right]. \tag{13}$$

At $(Hw)^2 \ll B$ the intensity change is $\Delta I_s \sim T'(Hw)^2$ and is
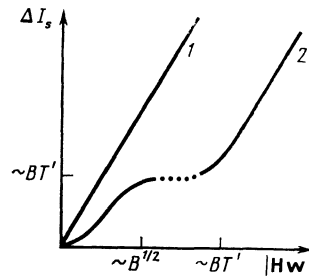
FIG. 2. US contribution $\Delta I_s(Hw)$ to the diffraction intensity in a weakly deformed crystal $(I_d \approx I_0)$: $1 - B^{1/2}T' \ll 1$; $2 - BT' \ll 1 \ll B^{1/2}T'$.

independent of the deformation parameter B. If $(Hw)^2 \gg B$, then ΔI_s reaches saturation. The value of ΔI_s remains small ($\Delta I_s \ll I_0$) but is much larger than the increase $\Delta I_d \sim (BT')^2$ of the scattering intensity as a result of the static deformation. For $Hw > BT'$ one must use the asymptote (10), and the influence of the US on the diffraction is practically the same as in the case of an undistorted crystal (Fig. 2).

3. $BT' \gg 1$. In the absence of US, the scattering intensity I_d becomes much higher than I_0:

$$\frac{I_d}{I_0} \approx \frac{4}{\pi}\frac{BT'}{\cos\theta_B} = \frac{4BT}{\tau} \gg 1. \tag{14}$$

The incident wave excites points 1 and 8 on the DS (Fig. 1a) in a region of width $\sim BT'$ mainly outside the principal $\Delta\theta_0$ maximum. Point 1 follows the path 1-2-3-4 and is transformed into a state corresponding to a diffracted wave (the direction of the group-velocity vector, the normal to the DS, almost coincides with $\mathbf{k}_h$). The direction of motion of the point 8 is such that it can make no contribution to the diffraction.

Let us examine in greater detail the influence of the US wave. The US hardly perturbs the motion of the point 8, and its contribution to the diffracted wave is close to zero. A diffracted wave is produced as before if the point 1 lands in the state 4, but now it can follow two paths: 1-2-6-7-3-4 (probability (M_1^2)) and 1-2-3-4 (probability R_1^2). (The interference between the processes 2-6-7-3 and 2-3 is discussed in Sec. 2.3.) The intensity change ΔI_s following application of the US is thus

$$\Delta I_s/I_d = R_1^2 + M_1^2 - 1 = -2R_1 M_1 < 0. \tag{15}$$

It follows from (15) that weak US, $(Hw)^2 \lesssim B$, can lower the scattering intensity by as much as 50% ($R_1 = M_1 = 0.5$). For $(Hw)^2 \gg B$ we have $\Delta I_s \approx 0$, i.e., one-photon processes cease to influence the diffraction. Recall that in an ideal crystal the situation is entirely different: in the $Hw \ll 1$ approximation the US enhances I, but its influence is much weaker: $\Delta I_s/I_0 \sim Hw$ (Ref. 4).

2.2. Multiphonon processes

As the excitation point moves over the DS it passes through sections where n-phonon transitions are substantial. Using the expansion[17]

$$\exp[2iHw\sin(k_s z - \omega_s t)] = \sum_{n=-\infty}^{\infty} J_n(2Hw)\exp[in(k_s z - \omega_s t)],$$

$$\tag{16}$$

where J_n is a Bessel function of order n, we find [just as in the derivation of (15)] the probabilities of going over to another DS sheet (M_n) or of staying in the initial state (R_n) for an n-phonon process:

$$R_n = \exp(-\pi F_n^2/2B), \quad M_n = 1 - R_n,$$

$$F_n = J_n(2Hw) \sum_m [g^{-1/4}\delta_{n,2m+1} + g^{1/4}\delta_{n,2m}], \quad (17)$$

$$g = 1 - [2J_0(2Hw)/n\Omega]^2.$$

If $Hw > B^{1/2}$ the one-phonon processes no longer influence the diffraction intensity I, while two-phonon processes still have low probability. At $Hw \sim B^{1/4}$ two-phonon processes decrease I (to 50%), next ($Hw > B^{1/4}$) they "go out of play," followed by the onset of three-phonon transitions, etc. Thus, the $I(Hw)$ plot should reveal multiphonon oscillations (Fig. 3). Since the influnce of an n-phonon process is strongest at $Hw \sim B^{1/2n}$, in the limit as $n \to \infty$ there is a point where the oscillations condense, and their contrast decreases. We emphasize that in a deformed crystal multiphonon processes make a noticeable contribution to I even in weak US fields ($Hw \ll 1$), whereas in an ideal crystal they "work" only if $Hw > 1$.

Let us consider the case $Hw \gg 1$. Using the asymptotic expressions for $J_n(2Hw)$ we obtain after laborious calculations[16]

a) $T' \gg Hw \gg 1$

$$I/I_d \approx 0.5 + 2Hw/N, \quad N = 4BT'/\Omega \cos\theta_B, \quad (18)$$

(b) $Hw \gg T'$

$$I_\infty = I_d \pi/2B, \quad (19)$$

i.e., the scattering intensity reaches the kinematic limit (Fig. 3). The first term on the right hand side of (18) results again in a 50% decrease of I, while the second corresponds to a situation in which the excitation point moves over the DS and lands in succession in places where transitions of multiplicity $n \lesssim 2Hw$ are possible. We emphasize that although that part of $I(Hw)$ which is linear in Hw is independent of the strain parameter B, the scattering proceeds in a manner different than in an ideal crystal in which $I \sim (Hw)^{1/2}$ in this limit[18] (this corresponds to immobile DS excitation points).

2. 3. Interference beats induced by US

A crystal strain $BT' \sim 1$ suppresses both the ordinary scattering-intensity oscillations connected with the gap Δk_0
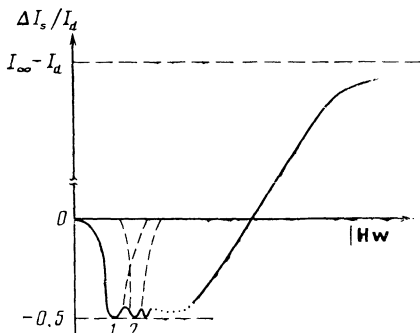
FIG. 3. Relative US contribution $\Delta I_s/I_d$ in a strongly distorted crystal ($I_d \gg I_0$).

and the US beats due to the gaps Δk_s. We shall show, however, that interference beats of a new type occur in a deformed crystal (including the case $BT' \gg 1$).

We confine ourselves to the case $(Hw)^2 \ll B$, when the most substantial are the one-phonon transitions. We assign purely formally to the DS sheets the quantum numbers $\sigma_z = -1$ (for the upper branch) and $\sigma_z = 1$ (for the lower). We consider in greater detail the dynamics of the representative point 1 (Fig. 1a). Moving adiabatically over the DS $\sigma_z = 1$, it reaches the position 2 and can subsequently remain on the sheet $\sigma_z = 1$ or, absorbing a phonon, go over to position on the sheet $\sigma_z = -1$. The beams corresponding to 2 and 6 propagate along different spatial trajectories (Fig. 1b) and, after covering the distance ΔS_0 (7) they stop at one and the same place in the crystal, but at points 3 and 7 on the DS. After emission of a US phonon, the representative point goes over from the sheet $\sigma_z = -1$ to the sheet $\sigma_z = 1$. The amplitudes of the processes corresponding to the paths 2–3 and 2–6–7–3 interfere. The phase changes φ_{23} and φ_{67} are of the form

$$\varphi_{23} = -\varphi_{67} = \frac{\beta\Omega a}{4B} - \frac{1}{4B}\ln\frac{\beta\Omega+a}{\beta\Omega-a},$$

$$\beta = \pm 1, \quad a = \left[\left(\frac{\Omega}{2}\right)^2 - 1\right]^{1/2}. \quad (20)$$

In analogy with (15), we find the change produced in the diffraction intensity by the US:

$$\Delta I_s/I_d \approx -2R_1 M_1 [1 - \cos(2\varphi_{23})], \quad (21)$$

which is an oscillating function of the parameter B^{-1}. For each radiation phonon incident on the crystal, the points corresponding to the transitions 6–2 and 3–7 retain their spatial coordinates, but the distance ΔS_0 between them along the k_0 direction and the phases φ_{23} and φ_{67} are determined only by the US frequency and are independent of the momentum P_h. There is therefore no mutual extinction of these oscillations in a strained crystal, in which the scattering intensity is considerably higher than in an ideal one, and the ordinary Pendellösung beats are already suppressed. These interference phenomena do not take place, naturally, in a perfect crystal.

3. EXPERIMENTAL RESULTS

3.1. Neutron diffraction

We used for the measurements a neutron diffractometer[19] mounted on the horizontal channel of the IRT-M reactor of our Institute. The sample was a dislocation-free silicon single crystal 70 mm in diameter and $T = 1.73$ mm thick (the same as used in Ref. 6). We investigated the reflection ($2\bar{2}0$) in a Laue-symmetry reflection geometry. A transverse US wave ($k_s \pm H$, $w \| H$) was excited with of a quartz piezoconverter (Y-cut) secured to the sample by epoxy resin without a hardener. We used the third harmonic ($\nu_s = 56.4$ MHz), to be able to work far from the lower threshold frequency $\nu_{th\,1} = 14.7$ MHz and disregard, in contrast to Ref. 6, the interband interference of the Bloch state in the undeformed crystal. The sample was deformed by a simple bending device (by pressing two sections of the plate to an annular holder). A beam of monochromatic neutrons ($\lambda = 1.01$ Å) of 4×2 mm cross section was scattered in the
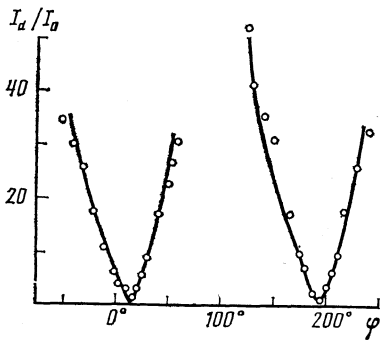
FIG. 4. Normalized diffraction intensity $I_d(\varphi)/I_0$ in a strained plate vs the angle φ. The two measurement runs (circles) differ by a rotation through $\Delta\varphi = 180°$. The solid lines were calculated from (23) for $A' = 30$ and $\alpha = 15°$.

central part of the plate. The holder with the sample was secured in an STF-1 goniometer attachment, which made it possible to tilt the crystal by an arbitrary angle φ around an axis parallel to the vector **H**. This changed the effective sample thickness to $T_e = T/\cos\varphi$, leading to Pendellösung beats of the diffraction intensity $I(\varphi)$ (the tilting method of Ref. 20). We observed such beats in an unstrained plate.[6] Under even a weak strain, however, the thickness oscillations vanished and were replaced, at a tilt angle $\varphi \sim 50°$, by 30–40-fold increase of $I(\varphi)$ (Fig. 4). These data can be used to estimate the strain gradients on the basis of quasiclassical theories.[12-14]

As already indicated, in the case of smooth static strains the atomic displacements are described by a quadratic function (3) of the coordinates s_0 and s_h. Transforming to a coordinate frame connected with the tilted crystal, we obtain in the lab, after simple calculations (see also Ref. 21), the φ dependence of the parameter B of the strain gradient in the scattering plane:

$$B = A \sin(\varphi + \alpha), \tag{22}$$

where A and α are certain constants. Next, using (14) and (22), we obtain the dependence of the normalized diffraction intensity on φ:

$$\frac{I_d}{I_0} \approx \frac{4BT_e'}{\pi \cos\theta_B} = A'\frac{\sin(\varphi + \alpha)}{\cos\varphi}, \quad A' = \frac{4}{\pi}\frac{AT'}{\cos\theta_B}. \tag{23}$$

At values $A' = 30$ and $\alpha = 15°$ Eq. (23) describes the experimental data well (Fig. 4). A better idea of the quality of the fit is gained from Fig. 5, which shows the linear (except in the region of smallest B) dependence of I_d/I_0 on B. The values of B calculated from (23) lie in the range $0 \lesssim B \leqslant 0.6$. The maximum sample strain was $\delta \approx bT/H \approx 10^{-5}$, corresponding to a flexure radius $R \approx 100$ m.

The subsequent measurements were made under conditions of US excitation. Figure 6 shows plots of the diffraction intensity vs the piezoconverter voltage $V \sim Hw$ at different values of φ. The characteristic features of these plots agree with the main conclusion of the theory expounded in Sec. 2.

1. For large Hw ($V \approx 3$–5 V), I is linear in $V \sim Hw$, with the lines having equal slopes in a wide range of ($0.08 \lesssim B \lesssim 0.6$).

2. The slopes of lines 2–6 for a strained crystal differ substantially from the slope of $I(V)$ for a perfect crystal (cf., e.g., curve 2, for which B is only 0.03, and curve 1, where $B \approx 0$).
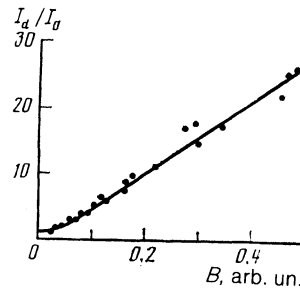
FIG. 5. Normalized diffraction intensity I_d/I_0 vs the strain parameter B in the absence of US. Points—values of B calculated from the experimental $I_d(\varphi)$.

3. For relatively large strains ($B \gtrsim 0.1$, curves 4–6), a noticeable decrease of the scattering intensity is observed on the initial sections of the $I(V)$ plots,[22] and the depth of the falloff and its length in terms of V depend on the parameter B.

4. Oscillations in the falloff regions are observed on curves 4–6 and their contrast is higher for small values of B.

Let us compare in greater detail the experimental data with the theory. We note as a preliminary that the US wave excited in the crystal is usually a standing one and can be represented as a sum of two traveling waves with $\pm k_s$. In neutron diffraction, in view of the substantial role of energy exchange between the neutron and the US phonons, the two traveling waves will be subject to different threshold conditions[4] that can be described by the common equation
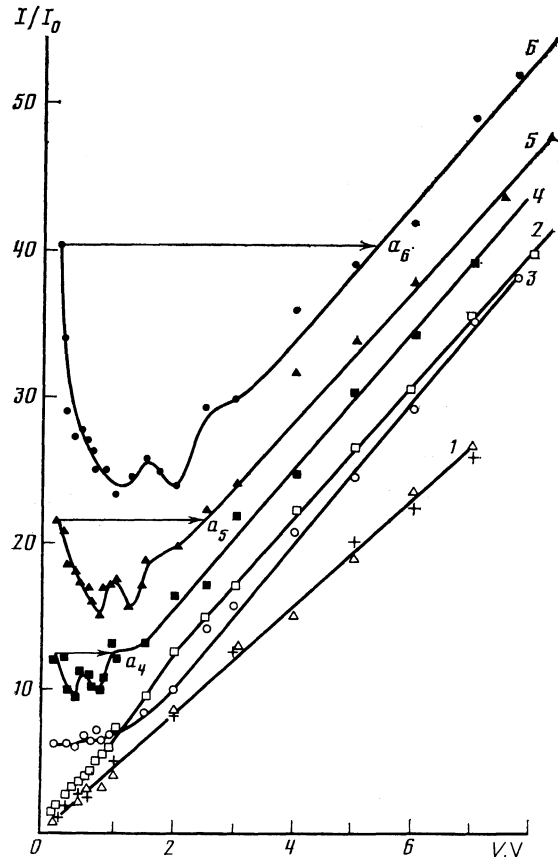
FIG. 6. Normalized diffraction intensity I/I_0 vs the voltage V at different values of φ: 1—unstrained plate, $B = 0$, two measurement runs corresponding to $\varphi = 0$ and $\varphi = 45°$; strained plate: 2—$B = 0.03$; 3—$B = 0.08$; 4—$B = 0.19$; 5—$B = 0.29$; 6—$B = 0.49$. a_i—points of "return" ($i = 4, 5, 6$) of the $I(V)/I_0$ dependence to the zero level $I(0)/I_0$.

$$\frac{\Omega_\pm}{2} = \frac{k_s}{\Delta k_0}\left(\frac{v_s}{v_n \cos\theta_B} \pm \cos\varphi\right) = 1, \qquad (24)$$

where v_s is the US wave velocity. For Si(2$\bar{2}$0) and $\lambda = 1.01$ Å we have $v_{th\,1} = 14.7$ MHz and $v_{th\,2} = 101$ MHz. Since experiment gives $v_{th\,1} < v_s = 56.4$ MHz $< v_{th\,2}$, only one type of DS crossing need be considered in the case of a perfect crystal, and according to Refs. 4 and 5 we have

$$I/I_0 \approx 1 + K_0 Hw, \qquad K_0 = 4. \qquad (25)$$

The situation for a strained crystal is more complicated, since a major role is played by multiphonon processes and both limiting frequencies must in fact be taken into account in the region $Hw \gtrsim 1$. At $Hw \gg 1$ and $BT' \gg 1$ we obtain, with (14), (18), and (24) taken into account,

$$I/I_0 \approx 0.5 I_d/I_0 + K_d Hw, \qquad K_d = 2(\Omega_+ + \Omega_-)/\pi. \qquad (26)$$

Substituting expression (24) for $\Omega_\pm$ we find ultimately that

$$K_d = \frac{8}{\pi}\frac{k_s v_s}{\Delta k_0 v_n \cos\theta_B} \qquad (27)$$

and is independent of the angle φ, i.e., of B. The ratio

$$\frac{K_d}{K_1} = \frac{2}{\pi}\frac{k_s v_s}{\Delta k_0 v_n \cos\theta_B} \qquad (28)$$

for real parameters is $K_d/K_0 = 1.41$. Analysis of the experimental data (Fig. 6) shows that the slopes of the linear sections of the $I(V)$ plots (at large V) are indeed independent of B, in accordance with (27), and the ratio of the slopes of curves 3–6 to the slope of curve 1 (perfect crystal), $(K_d/K)_e = 1.55 \pm 0.10$, is in fair agreement with the value calculated with the aid of (28). We obtain, in passing, from the slopes of plots 1–6 a calibration relation for Hw as a function of V:

$$Hw = (0.95 \pm 0.10)V. \qquad (29)$$

In the region of small US displacements ($Hw \ll 1$) the scattering features are determined mainly by one-phonon processes. In particular, the observed anomalous behavior (decrease) of $I(V)$ is due to transitions of the excitation points between the DS sheets, i.e., to violation of the adiabaticity conditions. This situation is realized only for relatively large strains $B > B_{tr}$, where

$$B_{tr} = \frac{\cos\theta_B}{T'}\left[\left(\frac{\Omega}{2}\right)^2 - 1\right]^{1/2} \approx \frac{\Omega}{\Delta k_0 T}, \qquad v_s \gg v_{th}. \qquad (30)$$

If $B > B_{tr}$, the $I(V)$ plots should have descending sections. At $B < B_{tr}$ the US increases $I(V)$. The condition (30) arises physically when the change of the component of the neutron
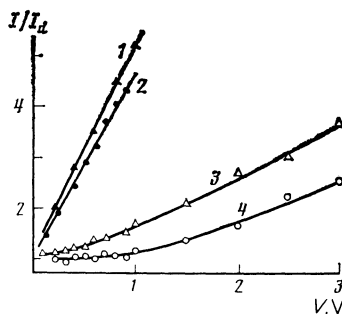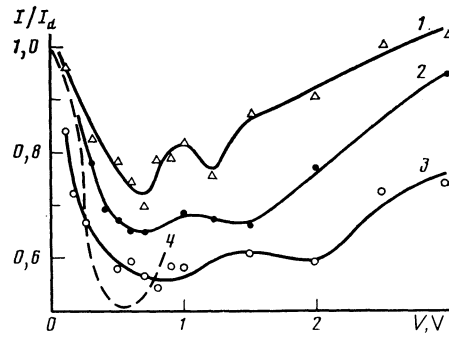
FIG. 8. Falloff of normalized diffraction intensity $I(V)/I_d$ in the case of relatively high strain ($B > B_{tr}$) under US excitation. Experimental data 1—$B = 0.19$; 2—$B = 0.29$; 3—$B = 0.6$. Dashed line 4—calculation of the position of the first minimum with the aid of (12) and (15).

momentum along the x axis ($P_0 - P_h + 4BS_0$) becomes equal, on passing through the crystal, to the distance (in momentum space) between the vicinities of the transitions 2–6 and 3–7 (see Fig. 1).

Figures 7 and 8 show in detail the region of small V for the measured $I(V)$ curves. It can be seen that there exists indeed a limiting value of the parameter $B = B_{tr}$, which separates regions with qualitatively different behaviors of $I(V)$. The foregoing experimental data yield the estimate $B_{tr} \approx 0.13$, which is close enough to the value $B_{tr} \approx 0.11$ obtained with the aid of (30).

The most difficult to analyze are the experimental data in the intermediate region $Hw \sim 1$ of US displacements, since the analytic expressions for $I(Hw)$ in Sec. 2 were obtained only for a few limiting cases. Nonetheless, a number of qualitative conclusions of the theory can be verified. Thus, using the asymptote (26) for $I(V)$ plots with falloff, we obtain the relation between the quantity $\eta_{min} = 0.5 I_d/I_0$ (the minima of the $I(Hw)$ curves) and the "return" point $|Hw|_a$ of the $I(Hw)$ intensity on the zeroth level $\eta = I_d/I_0 \equiv I(0)/I_0$:

$$\eta_{min} = K_d|Hw|_a. \qquad (31)$$

Larger values of η_{min} correspond to "farther" return points $|Hw|_{a_i}$, as is indeed observed in experiment (Fig. 6). Reducing the plots 4–6 of Fig. 6 with the aid of (31), we obtain an independent calibration $V(Hw)$ that should coincide with (29). Recognizing that η_{min} is determined from the experimental data with not too high an accuracy (since it is necessary to average over the oscillations), the agreement between the calibrations (Fig. 9) can be regarded as satisfactory.

FIG. 7. Growth of normalized diffraction intensity $I(V)/I_d$ in the case of small strains ($B < B_{tr}$) under US excitation 1—$B = 0$; 2—$B = 0.03$; 3—$B = 0.08$; 4—$B = 0.13$.
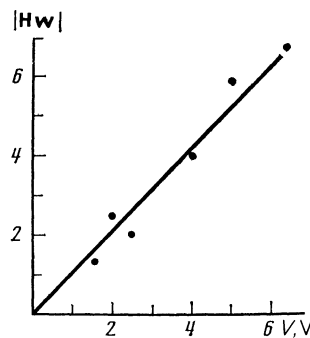
FIG. 9. Calibration dependence of $|H \cdot w|$ on the piezo-converter voltage V. The points were obtained from (31) and the solid straight line corresponds to (29).

With increase of V in a strained crystal, a more noticeable influence is exerted on the diffraction by multiphonon processes that lead to oscillations of the intensity $I(V)$ in the region of the minimum. At least two oscillations appear on each of the curves 4–6 of Fig. 6 (cf. Fig. 3). The depth of the oscillations and the positions of the minima depend on B. It follows from the theory that a US wave can lower the scattering intensity I by 50% [see Eq. (15)]. A decrease of I by almost 50% is indeed observed, but only under relatively strong strains ($B \approx 0.5$–0.6). The experimental depth of the dip depends on the parameter B, a fact not reflected in the approximate calculations. Expressions (12) and (15) do nevertheless describe correctly the $I(V)$ dependence also in the intermediate region $Hw \sim 1$ (see curve 4 of Fig. 8).

We note in conclusion that the incomplete quantitative agreement between the theory and the experimental data is due, on the one hand, to the asymptotic character of the calculations, and on the other to the influence of the inhomogeneities of the sound field (in the cross sections of the incident and reflected neutron beams) on the measurement results.[5]

3.2. X-ray diffraction

The measurement were performed with a DRON-3 diffractometer in Mo $K\alpha$ radiation. The sample was a plate of KDB-10 silicon [(111) orientation] 76 mm in diameter and $T \approx 360\,\mu$m thick. We investigated the symmetric reflection (660) in Laue geometry. One surface of the plate was ground, and to the other, after chemical and mechanical polishing, was glued (with epoxy resin and without hardener) a quartz piezoconverter (Y cut). The transverse US wave ($\mathbf{k}_s \perp \mathbf{H}$, $\mathbf{w} \| \mathbf{H}$) was excited at the third harmonic ($\nu_s \approx 60$ MHz $\gtrsim \nu_{th} \approx 57$ MHz).

Slight pressure on the holder produced in the Si crystal an inhomogeneous strain field. Some idea concerning this field can be gained from Fig. 10, which shows the dependence of the diffraction intensity $I_d(x)$ obtained by scanning (without US) the plate along the vector $\mathbf{H}$ (the x axis). The intensity of the diffraction by the unstrained plate was of the order of $I_0 = 30 \cdot 10^3$ counts/10 s. Thus, the largest strains that lead to a growth of I_d are concentrated in a region of $x \approx 50$ mm, and the largest near $x \approx 30$ mm and $x \approx 0$. According to the theoretical premises of Sec. 2, the effect of US on x-ray diffraction in these regions should differ noticeably,
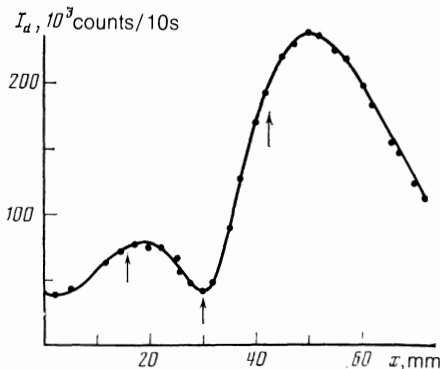
FIG. 10. X-ray diffraction intensity I_d in a strained Si plate. Diametral scanning. The arrows show the sections subsequently investigated under US excitation conditions.
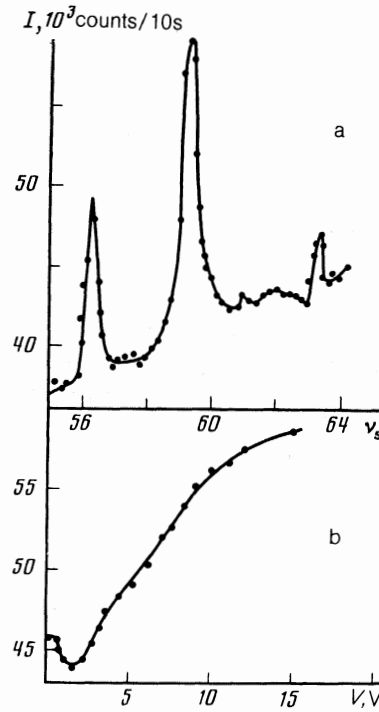
FIG. 11. Frequency $I(\nu_s)$ (a) and voltage-count $I(V)$ (b) dependences of the diffraction intensity I at the point $x = 30$ mm.

since they have substantially different values of the parameter $B \approx I_d \tau / 4 I_0 T$ [see Eq. (14)]. By way of example, we present the experimental data for the points $x = 30$ mm ($B \approx 0.095$) and $x = 42$ mm ($B = 0.46$). [Equation (14) is valid at $I_d \gg I_0$, therefore the estimate of B at the point $x = 30$ mm is quite approximate.] Figures 11 and 12 show the corresponding dependences of the diffraction intensity I on ν_s ($V = $ const) and on V at a fixed frequency ν_s. The $I(\nu_s)$ curves have a distinct structure due to excitation of natural resonances in an acoustic system consisting of the piezoconverter, the glue, and the Si plate. The most interesting feature is the observed inversion of the frequency spectra obtained upon diffraction by the strained region of $x = 42$ mm relative to the almost perfect region of $x = 30$ mm. The dips in Fig. 12a illustrate clearly the anomalous influence of the US on the diffraction in a strained crystal. More detailed information yield the $I(V)$ plots measured at the frequency of the central resonance (Figs. 11b and 12b). In the strained regions, the US decreases $I(V)$, and furthermore stronger the larger the strain gradient (the decrease amounts to 18% at $x = 16$ mm and 25% at $x = 42$ mm). These qualitative features agree with the theory (Sec. 2).

Let us discuss some specific aspects of x-ray diffraction under US excitation conditions. Since the x-ray photons pass through the crystal in a time $t_0 \sim 10^{-12}$ s, the scattering intensity I represents the instantaneous atomic-position distribution modulated by excitation of a standing US wave. The change of the scattering intensity in a strained crystal at the instant of time t (in the one-phonon approximation) is described by expression (15), where R_1 is replaced by R_t:

$$R_t = \exp\left[-\frac{\pi (Hw)^2 \sin^2(\omega_s t)}{2B[1-(\Delta k_0/k_s)^2]^{1/2}} \right]. \tag{32}$$

The time-averaged value $\bar{I}(Hw)$ measured in experiment is given by

$I, 10^3$counts/10s

220 ─

200 ─

180 ─

        a

|56|60|64| v_s

210 ─

190 ─

        b

|5|10|15| V, V
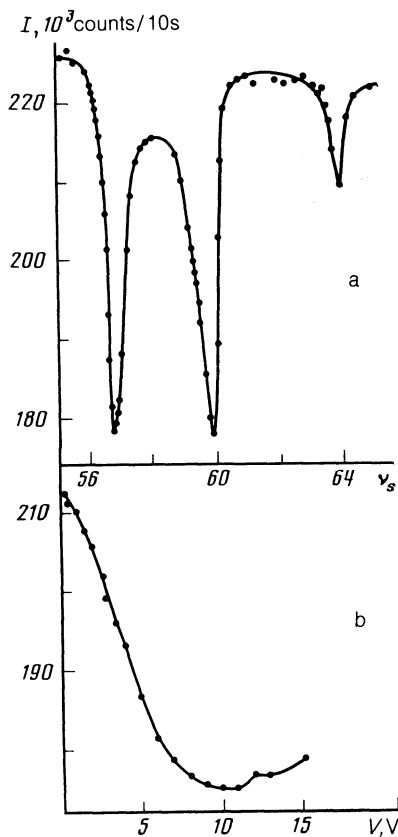
FIG. 12. The same as Fig. 11, but at the point $x = 42$ mm.

$$\bar{I}/I_d = 1 - 2\lceil e^{-\tau}Y_0(\gamma) - e^{-2\tau}Y_0(2\gamma)\,\rceil,$$

$$\gamma = \frac{\pi}{4B}(Hw)^2\left[1 - \left(\frac{\Delta k_0}{k_s}\right)^2\right]^{-\frac{1}{2}}, \qquad (33)$$

where Y_0 is a modified Bessel function.

It follows from (33) that the maximum possible decrease of $\bar{I}/I_d$ in the case of x rays is already 35%, and the $\bar{I}(Hw)$ dependence is a smoother function of $Hw \sim V$ than in neutron diffraction, as is indeed observed in experiment. The weaker influence of US on x-ray diffraction is qualitatively due to the fact that the amplitude of the displacements in a standing wave is zero at definite instants of time. Recall that for neutron diffraction the US waves traveling in opposite direction ($\pm k_s$) cause intersections at different points of the DS and their contributions to scattering must be taken into account individually.

A detailed quantitative comparison with experiment is as yet difficult, since the x-ray experiment was performed at frequencies close to threshold, and this situation, as is well known,[6] requires a special theoretical analysis.

4. CONCLUSION

The influence of smooth static strains (not connected with US) on the diffraction of rays in single crystals was the subject of many studies. Particular attention was paid to the dynamics of the motion of the excitation points over the DS. It has been shown[14] that the adiabaticity of the motion is violated at $B \gtrsim 1$, i.e, transitions between sheets of the DS take place. Under US excitation, the role of the adiabaticity parameter is assumed by the quantity $B/(Hw)^2$ (at $B > B_{tr}$). By varying B and the amplitude w of the US

wave in the crystal, we were able to track theoretically and experimentally the transition from the regime of nonadiabatic action of the US to the regime of adiabatic motion of the excitation point over the DS reconstructed by the US. This leads to various manifestations in the behavior of the integral scattering intensity I, which differs substantially from the case of a perfect crystal.

In relatively strongly distorted crystals, when I_d is several times larger than I_0, an anomalous $I(Hw)$ dependence is observed. At small Hw the high-frequency sound decreases $I(Hw)$, a substantial role is assumed by multiphoton processes, and only with further increase to $Hw > 1$ does the diffraction intensity begin to increase linearly. The action of weak US on diffraction is numerically (in absolute units) more noticeable in a strained crystal than in an ideal one. We have shown that the decrease of $I(Hw)/I_d$ can reach 50%. The reason is that in the presence of a strain gradient the excitation point moves over the DS and under certain conditions [Eq. (30)] it finds automatically the "action zone" of the US. In other words, the kinetics of the motion over the DS is of decisive significance. In a perfect crystal, the US influences strongly only those immobile excitation points that can become intermixed by the US perturbation.

In a strained single crystal, when the usual extinction beats are already absent, the theory predicts the existence of a new type of Pendellösung beats on passage of radiation beams through the crystal under US excitation conditions. Reliable observation of such "strain" beats calls for special experiments.

On the whole, the investigations suggest that between the usual mosaic crystals, in which US has practically no effect on the diffraction, and perfect ones, where the diffraction intensity behaves in normal fashion (increases) under US excitation, there exists an extensive region of smoothly strained crystals in which US exerts a strong anomalous influence on the scattering of neutrons and x rays.

[1] For x rays, v_{th} is determined from the condition $\lambda_x = \tau$. In the case of neutrons, the threshold condition is somewhat altered[4] by the need for taking into account the energy exchange between the neutron and the US phonons (see Eq. (24) below).

[1] W. Spencer, in: Physical Acoustics, W. P. Mason ed., Vol. 5, Academic, 1968.

[2] B. Buras, T. Giebultowicz, M. Minor, and A. Rajca, Phys. Stat. Sol. (a) 9, 42 (1972).

[3] I. R. Entin, Zh. Eksp. Teor. Fiz. 77, 214 (1979) [Sov. Phys. JETP 50, 110 (1979)].

[4] E. M. Iolin and I. R. Éntin, ibid. 85, 1692 (1983) [58, 985 (1983)].

[5] É. V. Zolotyabko, E. M. Iolin, V. I. Kuvaldin, et al. Preprint ALFI-064, Phys. Inst. Latv. Acad. Sci., 1984.

[6] E. M. Iolin, É. V. Zolotoyabko, E. A. Raïtman, et al., Zh. Eksp. Teor. Fiz. 91, 2132 (1986) [Sov. Phys. JETP 64, 1267 (1986)].

[7] I. R. Entin and I. A. Puchkova, Fiz. Tverd. (Leningrad) 26, 3320 (1984) [Sov. Phys. Solid State 26, 1995 (1984)].

[8] K. P. Assur and I. R. Entin, ibid. 24, 2122 (1982) [24, 1209 (1982)].

[9] B. Chalupa, R. Michalec, L. Horalik, and P. Mikula, Phys. Stat. Sol. (a) 97, 403 (1986).

[10]I. R. Entin, Pis'ma Zh. Eksp. Teor. Fiz. **26**, 392 (1977) [JETP Lett. **26**, 368 (1977)].

[11]R. Michalec, L. Sedlakova, R. Chualupa, *et al.*, Phys. Stat. Sol. (a) **23**, 667 (1974).

[12]P. Penning. Philips Res. Rep. Suppl. **21**, 1 (1966).

[13]V. L. Idenbom and F. N. Chukhovskiĭ, Usp. Fiz. Nauk **107**, 229 (1972) [Sov. Phys. Usp. **15**, 298 (1972)].

[14]F. N. Chukhovskiĭ, Metallofizika **2**, 3 (1980).

[15]S. Takagi, J. Phys. Soc. Jpn. **26**, 1239 (1969).

[16]E. M. Iolin, Preprint LAFI-102, Inst. Phys. Acad. Sci. Latv. SSR, 1987.

[17]I. S. Gradshtein and I. M. Ryzhik, *Tables of Integrals, Sums, Series, and Products*, Academic, 1965.

[18]I. R. Entin, Preprint Inst. Sol. St. Phys. USSR Acad. Sci., 1986.

[19]É. V. Zolotoyabko, E. M. Iolin, B. V. Kuvaldin, *et al.* Preprint LAFI-055, Phys. Inst. Latv. Acad. Sci., 1983.

[20]V. A. Somenkov, S. Sh. Shilstein, N. E. Belova, and K. Utemisov, Sol. St. Comm. **25**, 593 (1978).

[21]S. N. Voronkov, S. K. Maksimov, and F. N. Chukhovskiĭ, Fiz. Tverd. Tela (Leningrad) **26**, 2019 (1984) [Sov. Phys. Solid State **26**, 1225 (1984)].

[22]E. M. Iolin, E. A. Raĭtman, B. V. Kuvaldin, and É. V. Zolotoyabko, Sixth All-Union Conf. on Radiation Physics and Chemistry of Ionic Crystals, Abstracts, part II, Salaspils, Phys. Inst. Latv. Acad. Sci., 1986, p. 455.

Translated by J. G. Adashko